

ORIGINAL

## An Advanced Deep Learning Framework DeepLungNet with Global Average Pooling for Precise Lung Cancer Classification

Un marco de trabajo de aprendizaje profundo avanzado DeepLungNet con agrupación de promedios globales para una clasificación precisa del cáncer de pulmón

Savitha S<sup>1</sup>  , Kalai Vani Y S<sup>1</sup>  , Hridaynath Pandurang Khandagale<sup>2</sup>  , Umme Najma<sup>3</sup>  , Tirumalasetti Lakshmi Narayana<sup>4</sup>  , Jyothi N M<sup>5</sup>  

<sup>1</sup>BMS Institute of Technology and Management, Information Science and Engineering, Bengaluru, India.

<sup>2</sup>Shivaji University, Department of Technology, Kolhapur, India.

<sup>3</sup>Government Science College (Autonomous), Department of Biotechnology, Hassan, India.

<sup>4</sup>Aditya University, Electrical and Electronics Engineering, Surampalem, India.

<sup>5</sup>Koneru Lakshmaiah Education Foundation, Computer Science Engineering, Vaddeswaram, India.

**Citar como:** S S, Y S KV, Pandurang Khandagale H, Najma U, Lakshmi Narayana T, N M J. An Advanced Deep Learning Framework DeepLungNet with Global Average Pooling for Precise Lung Cancer Classification. Salud, Ciencia y Tecnología - Serie de Conferencias. 2025; 4:1551. <https://doi.org/10.56294/sctconf20251551>

Submitted: 27-08-2024

Revised: 08-11-2024

Accepted: 04-03-2025

Published: 05-03-2025

Editor: Prof. Dr. William Castillo-González 

Corresponding author: Savitha S 

### ABSTRACT

**Introduction:** lung cancer remains one of the deadliest diseases worldwide, with survival rates heavily dependent on early and precise detection. However, existing diagnostic methods face challenges in accuracy and efficiency. This research introduces DeepLungNet, an enhanced deep learning framework designed to improve lung cancer classification using Global Average Pooling (GAP). GAP is immensely important in reducing model complexity and overfitting, making it ideal for imaging in healthcare where datasets happen to be constrained. By preserving critical spatial information, it enhances model generalization and ensures reliable predictions.

**Method:** to develop a robust classification model, chest X-ray images were gathered from various origins, ensuring high diversity and quality. The dataset includes five categories: Bacterial Pneumonia, COVID-19, Normal, Tuberculosis, and Viral Pneumonia. DeepLungNet was evaluated against standard CNN architectures, including CNN, ResNet-50, and VGG16. The GAP layer proved instrumental in improving training efficiency, reducing computational overhead, and boosting classification accuracy. This makes it a strong candidate for real-world clinical deployment, particularly in resource-limited settings.

**Results:** DeepLungNet achieved 100 % accuracy, outperforming conventional models: CNN (93,40 %), VGG16 (94,25 %), and ResNet-50 (95,75 %). The model also attained perfect precision, recall, and F1-score, reinforcing its reliability in lung disease detection.

**Conclusion:** DeepLungNet demonstrates exceptional performance, making it a viable solution for accurate and efficient lung disease classification. Its 100 % accuracy and reduced computational demands make it ideal for clinical applications requiring fast, dependable diagnoses.

**Keywords:** Clinical Diagnostics; Lung Cancer; X-ray Imaging; Global Average Pooling; Medical Image Analysis; Early Disease Detection.

### RESUMEN

**Introducción:** el cáncer de pulmón sigue siendo una de las enfermedades más mortales en todo el mundo, y

las tasas de supervivencia dependen en gran medida de una detección temprana y precisa. Sin embargo, los métodos de diagnóstico existentes enfrentan desafíos en cuanto a precisión y eficiencia. Esta investigación presenta DeepLungNet, un marco de aprendizaje profundo mejorado diseñado para mejorar la clasificación del cáncer de pulmón utilizando Global Average Pooling (GAP). GAP desempeña un papel crucial en la reducción de la complejidad y el sobreajuste del modelo, lo que lo hace ideal para imágenes médicas donde los conjuntos de datos suelen ser limitados. Al preservar la información espacial crítica, mejora la generalización del modelo y garantiza predicciones fiables.

**Método:** para desarrollar un modelo de clasificación robusto, se recolectaron imágenes de rayos X de tórax de múltiples fuentes, lo que garantizó una alta diversidad y calidad. El conjunto de datos incluye cinco categorías: neumonía bacteriana, COVID-19, normal, tuberculosis y neumonía viral. DeepLungNet se evaluó en comparación con arquitecturas estándar de CNN, incluidas CNN, ResNet-50 y VGG16. La capa GAP demostró ser fundamental para mejorar la eficiencia del entrenamiento, reducir la sobrecarga computacional y aumentar la precisión de la clasificación. Esto lo convierte en un fuerte candidato para la implementación clínica en el mundo real, particularmente en entornos con recursos limitados.

**Resultados:** DeepLungNet logró una precisión del 100 %, superando a los modelos convencionales: CNN (93,40 %), VGG16 (94,25 %) y ResNet-50 (95,75 %). El modelo también alcanzó una precisión, recuerdo y puntuación F1 perfectos, lo que refuerza su fiabilidad en la detección de enfermedades pulmonares.

**Conclusión:** DeepLungNet demuestra un rendimiento excepcional, lo que lo convierte en una solución viable para la clasificación precisa y eficiente de las enfermedades pulmonares. Su precisión del 100 % y la reducción de las demandas computacionales lo hacen ideal para aplicaciones clínicas que requieren diagnósticos rápidos y confiables.

**Palabras clave:** Diagnóstico Clínico; Cáncer de Pulmón; Imágenes de Rayos X; Agrupación de Promedios Globales; Análisis de Imágenes Médicas; Detección Temprana de Enfermedades.

## INTRODUCTION

With a high death rate owing to late-stage diagnosis, still among the most often occurring and fatal forms of cancer worldwide is lung cancer. To improve treatment results and patient survival, lung cancer must be detected early.<sup>(1)</sup> Traditional diagnostic procedures have their uses, but they also have drawbacks that make it harder to catch problems early and drive-up healthcare expenditures. While imaging tests like computed tomography (CT), x-rays (X-rays), and biopsies are essential for diagnosing lung cancer, they are not without their drawbacks, such as the requirement for highly trained radiologists, variation in the interpretation of data, and lengthy wait periods for results.<sup>(2)</sup> Discrepancies in diagnosis and missing nodules, particularly in complicated or subtle situations, might arise from manual image processing performed by radiologists because of the heavy reliance on human judgment. Additionally, with the ever-increasing number of medical photographs in today's healthcare settings, manual examination becomes increasingly inefficient and time-consuming.<sup>(3)</sup> The conventional method of diagnosing lung cancer has traditionally placed a significant emphasis on the utilization of radiological imaging procedures like CT scans and chest X-rays. When doing a standard diagnostic procedure, a radiologist will look at medical images to determine whether there are any aberrant tissue patterns or visible lung nodules.<sup>(4)</sup> When it comes to the detection of malignancies in their early stages, CT scans are especially helpful because they produce high-resolution images that enable a complete examination of lung tissue. This manual inspection is highly subjective and predisposed to inaccuracy. There is a possibility that lung tumors that are irregularly shaped or tiny might be ignored, which would result in a delay in detection. Additionally, the growing quantity of imaging tests that need to be processed daily by healthcare institutions adds another layer of complexity to the workload that radiologists are expected to handle.<sup>(5)</sup> Medical diagnostics, particularly in lung cancer, started to investigate ML as a possible solution because of the rising complexity of data and the increasing demand for automation. As a substitute for more conventional approaches, ML models like RF, DT, and SVMs arose. These algorithms may detect lung cancer based on characteristics manually derived from medical images.<sup>(6)</sup> Feature extraction from images of lung nodules, such as their texture, edge, and form, was a primary focus of early ML-based systems. Classifiers were trained to distinguish between benign and malignant tumors using these features. The accuracy of ML approaches was much increased in comparison to the accuracy of previous manual methods; yet these systems still had substantial limits.<sup>(7)</sup> The process of manually determining significant image features was known as feature engineering. This procedure was not only time-consuming but also largely relied on the skill of the individual who carried out the work. In addition, conventional ML techniques frequently had difficulty generalizing adequately on complicated, high-dimensional data, such as medical imaging. This limited their capacity to attain the same degree of accuracy as human radiologists in situations that were established in the real world.<sup>(8)</sup> Among the most important changes occurring in the domain

of medical image analysis was the introduction of DL. It is no longer necessary to manually extract features when using deep learning, particularly when using CNNs.<sup>(9)</sup> However, DL enables the model to learn useful characteristics directly from the raw input. To overcome the constraints of typical machine learning models, this skill has shown itself to be one of the most successful. CNNs are ideally suited for image classification tasks such as lung cancer diagnosis because they automatically learn hierarchical features by applying convolutional filters to the images that they are processing.<sup>(10)</sup> To identify breast cancer, skin cancer, and lung cancer, CNNs are being employed successfully to several medical imaging problems. To be more specific, ResNet-50, VGG16, and Inception-v3 are examples of DL architecture that are widely utilized and have demonstrated remarkable performance in the process of identifying lung cancer.<sup>(11)</sup> Additionally, there are numerous parameters in the deep CNN models for model learning. We intend to develop the global average pooling layer to solve this problem by lowering the complexity and trainable parameters' influence. Literature surveys reveal that the capacity of ML algorithms, particularly DL, has attracted a lot of attention recently to recognize abnormalities in X-ray images. There have been several studies that have revealed favorable and accurate findings about the application of AI in medical research to aid diagnosis. Using AI and DNN, this article investigates the methods that previous researchers have utilized to treat lung-related illnesses effectively. A multiple-class classifier for the DL model is presented so as to detect lung cancer, pneumonia and COVID-19, by means of CT images and chest X-rays.<sup>(12)</sup> Given that the performance of four unique frameworks- blend of -Bi-GRU, VGG19, GRU and CNN with ResNet 152V2 the precision of the + CNN+VGG19 model was 88,05 %. Using VDSNet, CNN that connects with augmenting data and VGG, and a CNN with STN, the authors describe a unique hybrid DL architecture that they term VGG Data STN or VGG Data STN.<sup>(13)</sup> Vanilla Grey, added models like Vanilla RGB, hybrid CNN + VGG, and an amended Capsule Network were utilized in the development of the study. With a validation accuracy of 73 %, the VDSNet model that was proposed possesses. For detecting or identifying COVID-19, the authors employed SVM in conjunction with multi-level thresholding.<sup>(14)</sup> After looking at the patient's CRIs, the authors used a median filter to make the input CRIs more contrasty. The next step is to apply the Otsu objective function's ceiling for multiple levels picture differentiation. Afterwards, lungs both healthy and infected could be identified using the SVM. To classify CRIs, the work suggested a nine-layer DL architecture. Making use of a DL setup instructed from the ground up, six different datasets were acquired from publicly available CRIs.<sup>(15)</sup> Two-class categorization of three various illness categories- COVID- 19, pneumonia, and tuberculosis (TB)- was the aim. The authors used 6587 CRIs to train a DL model using stochastic gradient descent with 128×128 CRIs. For groups of CRIs, the model could fairly classify normal, TB, pneumonia, and COVID-19.<sup>(16)</sup> Applying the TL method and the famous CheXNet model, the COVID-CXNet was developed by the authors based on key characteristics and precise localization. The trustworthy model successfully identified new cases of COVID-19 pneumonia.<sup>(17)</sup> The authors used eleven convolutional neural network (CNN) models to categorize CRIs either normal, COVID-19, or patients with TB. They looked at three different ways to add further layers to the COVID-19 identification schemes.<sup>(18)</sup> All the models that were tested were popular frameworks that have been successful in picture detection and identification applications. After evaluating the suggested methods for each investigated design using a COVID-19 radiography database, the Xception and EfficientNetB4 models emerged as the best performers.

## METHOD

To improve chest X-ray picture reliant lung cancer grouping and forecasting, the suggested technique introduces a novel DeepLungNet architecture. A different dataset consisting of five separate categories was collected from various sources to commence the investigation. The proposed models are made up of the following sequences, as seen in figure 1:

The experiment is conducted in the following steps

1. Dataset Acquisition
2. Initial data preparation
3. Building DeepLungNet Framework with GAP Layer
4. Model Training
5. Model Test and Prediction

1. Dataset Acquisition: This study makes use of a dataset that includes 6,000 X-ray images of chest that have been classified into five groups: Healthy Lungs, COVID-19, pneumonia caused by bacteria, TB, and pneumonia by virus.<sup>(19,20,21,22,23,24)</sup> Images have been selected from several archives to guarantee variety and high quality. The sample image of all the categories and corresponding distribution is shown in figure 2.

As shown in table 1, for training, 80 % of the dataset (4800 pictures) is used with the remaining 600 pictures that is 10 % for validation and testing to build and evaluate our models. This data-splitting method keeps validation and testing sample sizes large enough while yet providing enough data for strong model training. A balanced and evenly distributed dataset was used to promote consistent and dependable model performance; each class had 120 validation images, 120 testing images, and 960 training images.

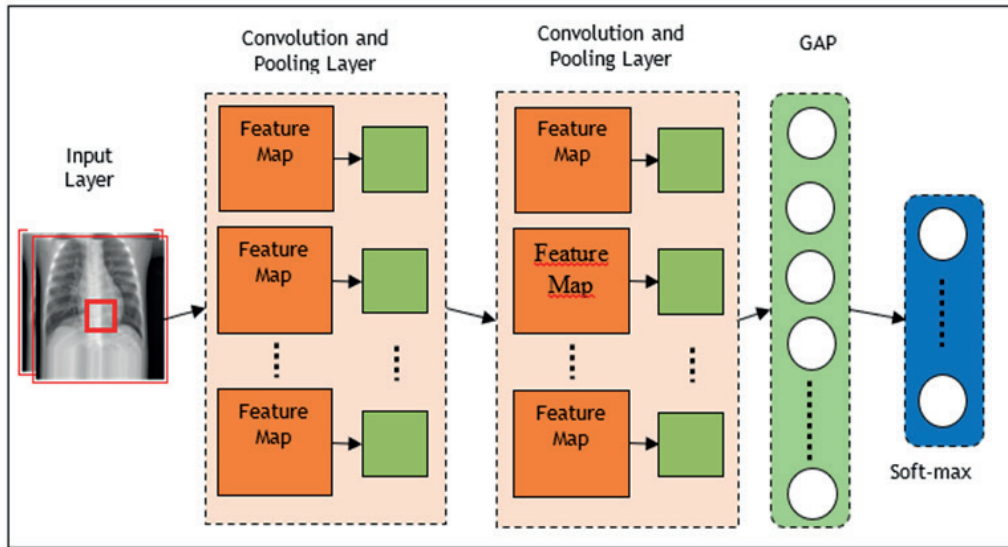


Figure 1. Architecture Diagram

2. Initial Data preparation: In this subsection, we used VisiPics to find and delete duplicate images, and then we used augmentation techniques to make sure the dataset was balanced across all classes by rotating, horizontally flipping, scaling, zooming, and adjusting brightness. To make sure each image could be used with the DeepLungNet model and make training as efficient as possible, we downsized them to 224x224 pixels.

Table 1. Lung Image dataset					
S. No.	Lung Image Class	Training	Validation	Test	Source
1	Bacterial Pneumonia	960	120	120	Chest X-Ray Images (Pneumonia) - Kaggle
2	COVID-19	960	120	120	COVID-19 Radiography Database - Kaggle
3	Normal Lungs	960	120	120	Chest X-Ray Images (Pneumonia) - Kaggle
4	Tuberculosis	960	120	120	Tuberculosis Chest X-ray Dataset - Kaggle
5	Viral Pneumonia	960	120	120	Chest X-Ray Images (Pneumonia) - Kaggle

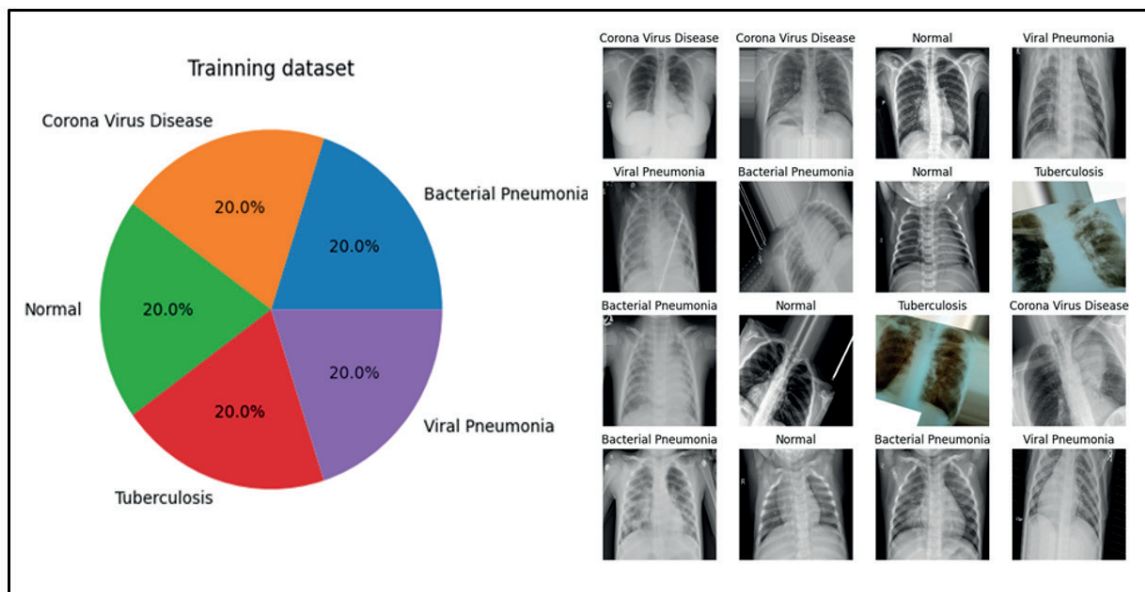


Figure 2. Sample Lung dataset and corresponding class distribution

3. Building DeepLungNet Model with GAP Layer: The DeepLungNet model has convolutional, pooling, GAP, and soft-max classifier layers. The convolutional layers of DeepLungNet automatically learn and extract spatial

information from chest X-ray samples. Individual filters scan the input image in small, limited areas and conduct convolution operations in these layers. After each convolutional process, the activation of ReLU helps to induce non-linear behavior. Using this stage, the network may simulate complicated data interactions by zeroing all negative values and maintaining positive values.

Next, max-pooling layers lower feature map spatial dimensions after convolutional layers. Using a 2x2 pooling window, the maximum pool chooses from every feature map, area with the highest value. This feature map down sampling prevents overfitting and computational complexity by lowering height and breadth while maintaining the most critical information. Max-pooling lowers feature map spatial size, hence improving network computing efficiency and decreasing sensitivity to small changes or distortions in input pictures, which is significant for medical imaging depicting lung disorders.

After the convolution and pooling layers, DeepLungNet presents an additional layer for Global Average Pooling (GAP). Finding the mean value for every feature map, the GAP layer reduces it to one single value unlike standard flattening methods that turn the whole feature map into a big 1D vector to feed into fully linked layers. In medical imaging, where global patterns like illness shape and distribution are crucial to proper classification, this decreases the number of parameters and maintains significant global context information about the image. For smaller datasets, DeepLungNet's GAP layer minimizes model complexity by omitting dense fully connected layers' many parameters.

4. Model Training: To provide faster convergence and increased performance, using the categorical cross-entropy loss function and configurable learning rate, the Adam optimizer oversaw the training process. When validation loss reached a point of saturation, a learning rate scheduler made real-time adjustments to the learning rate, allowing for even more efficient training. The training process was stabilized, and overfitting was prevented by using regularization techniques such as batch normalization, L2 regularization, and dropout layers. Using 100 epochs with 32-batch size the model is trained.

5. Model Testing and Prediction: To evaluate DeepLungNet, we used industry-standard performance measures to assess how well it performed on a distinct testing dataset that included all five classes.

## RESULTS

For training and testing, the proposed model was put through testing on a powerful machine that boasted NVIDIA, an Intel i9 CPU, 16GB of RAM, and a 1TB SSD for lightning-fast read/write operations. We used TensorFlow with Keras to build the models, plus NumPy, Pandas, OpenCV, Matplotlib, and Seaborn for processing images, managing data, and visualizing performance.

Measurements of performance: To assess the efficacy of the DeepLungNet model, several important metrics that are utilized to evaluate ML models for classification tasks, particularly those involving medical imaging are examined. We utilized the following metrics for this evaluation in equation 1 to 4:

Accuracy: It is the number of accurate forecasts—positive as well as negative—over the entire count of forecasts.

$$\text{Accuracy} = \frac{\text{Total Predictions}}{\text{Correct Predictions}} \quad (1)$$

Positive Predicted Value (PPV): Precision determines the number of the expected positive situations that turn out to be such. False positives are expensive to the model's efficacy measure, hence this statistic is rather helpful.

$$\text{Precision} = \frac{\text{Predicted Positive}}{\text{Predicted Positive and Correct}} \quad (2)$$

True Positive Rate (TPR): Recall is the number of the real positive cases the model accurately predicted. It underlines how well the model catches all positive cases.

$$\text{Recall} = \frac{\text{Actual Positive}}{\text{Actual Positive and Correct}} \quad (3)$$

F1-score (F1-s): If the class dispersion is unbalanced, the F1-score provides an integrated evaluation of recall and accuracy.

$$\text{F1-Score} = \frac{2 \times (\text{PPV} + \text{TPR})}{(\text{PPV} \times \text{TPR})} \quad (4)$$

## DISCUSSION

To provide accurate assessment, we used the same dataset, epochs, and model parameters to compare DeepLungNet's performance with classic frameworks like ResNet-50, CNN and VGG-16. We trained all the models for 20 epochs with the same batch sizes, learning rates, and other hyperparameters.

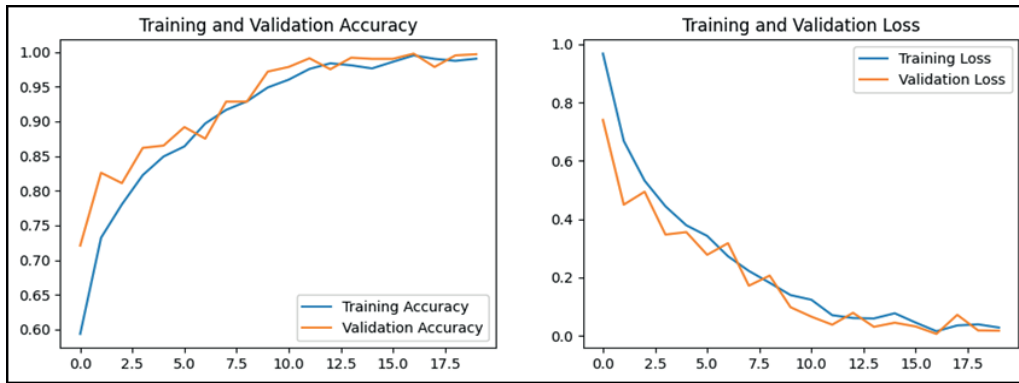


Figure 3. Accuracy of both validation, training and, Loss of suggested model

As shown in Figure 3, the superior validation accuracy for DeepLungNet suggests that the model generalizes better to unseen data, primarily due to the inclusion of the GAP layer, the generalizing ability of the system improves, and this allows to lower excessive fitting. DeepLungNet had the lowest training loss and validation loss, indicating more efficient learning compared to other models.

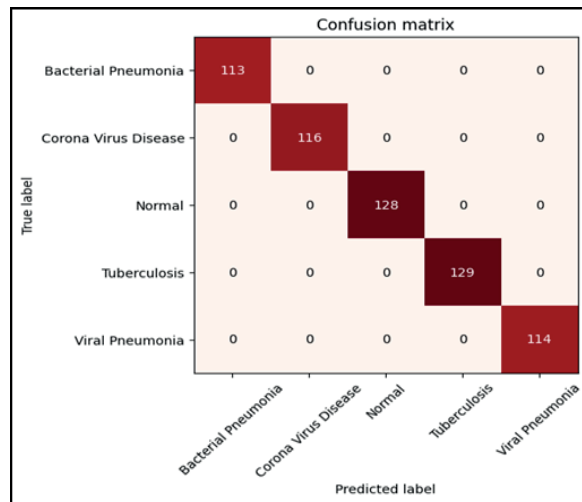


Figure 4. CM of proposed DeepLungNet model

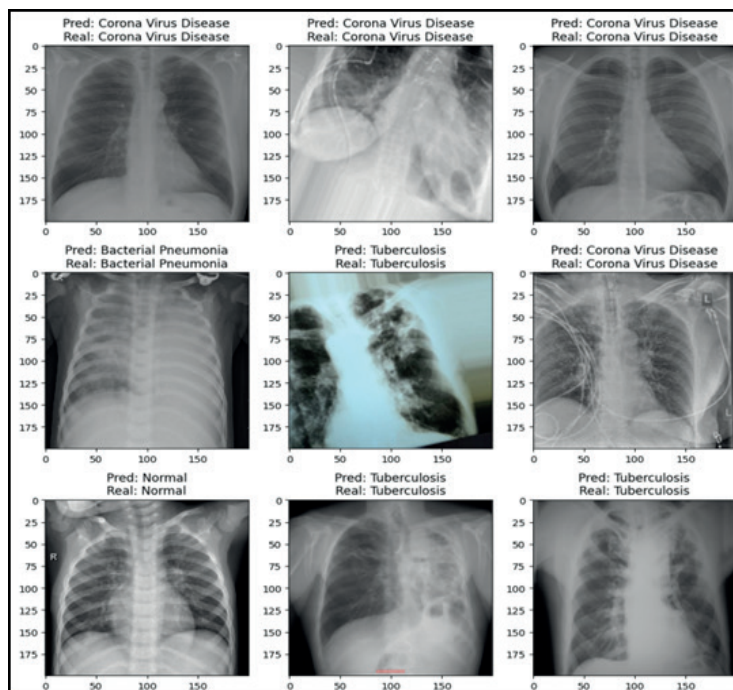


Figure 5. Prediction results of proposed model

Figure 4 of the confusion matrix shows that DeepLungNet did an outstanding task at lowering the false negative and positive counts. As an example, it obtained 113 instances of bacterial pneumonia correctly while it obtained zero false negatives. Similarly, when it came to COVID-19, DeepLungNet got 116 positive examples and misidentified none. The sample prediction of proposed work is shown in figure 5.

S. No.	Model	Acc.	PPV	TPR	F1- S
1.	CNN Model	93,40	93,15	93,25	93,20
2.	VGG-16 Net	94,25	94,10	94,45	94,25
3.	ResNet-50	95,75	94,50	94,25	94,75
4.	Proposed Model	100	100	100	100

When comparing DeepLungNet, CNN, VGG-16, and ResNet-50, it becomes clear that there are notable disparities in how effectively each model can identify lung disorders. As seen in table 2 and figure 6 DeepLungNet attained a 99,5 % accuracy rate for validation and a 100 % accuracy in training. In comparison, CNN, VGG-16, and ResNet-50 had lower training and validation accuracies.

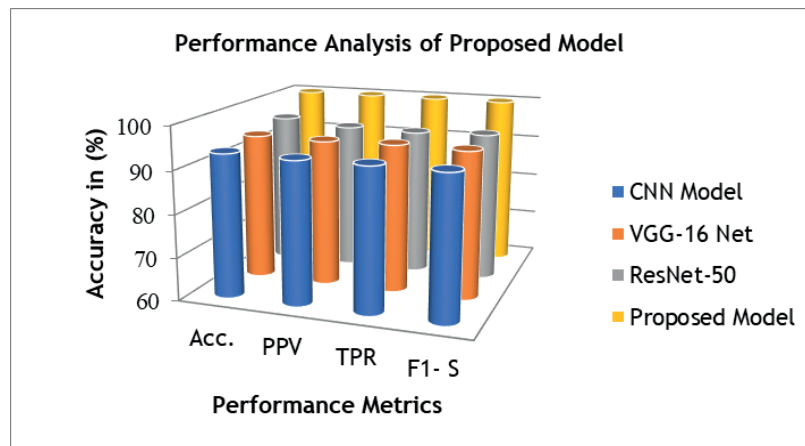


Figure 6. Performance Analysis of Proposed Model

## CONCLUSIONS

The fight against lung cancer demands innovative solutions that can surpass the difficulties of conventional diagnosis techniques. The development of DeepLungNet in this study demonstrates the power of advanced DL frameworks to transform healthcare. By incorporating GAP, DeepLungNet achieves a unique synergy of reduced complexity and preserves critical spatial information, paving the way for highly accurate predictions. The model was assessed using a comprehensive chest X-ray dataset containing five classes and demonstrated exceptional performance. DeepLungNet achieved an accuracy of 100 %, significantly outperforming traditional CNN architectures such as ResNet-50 and VGG16. Additionally, the GAP layer enabled faster convergence during training and reduced computational complexity.

## REFERECNES

1. Labaki WW, Han MK. Chronic respiratory diseases: A global view. *Lancet Respir Med.* 2020;8(6):531-3.
2. Bousquet J. *Global Surveillance, Prevention and Control of Chronic Respiratory Diseases.* Geneva: World Health Organization; 2007. p. 12-36.
3. *Global Initiative for Chronic Obstructive Lung Disease. Pocket Guide to COPD Diagnosis, Management and Prevention: A Guide for Healthcare Professionals.* Deer Park, IL: Global Initiative for Chronic Obstructive Lung Disease; 2021.
4. Palaniappan R, Sundaraj K, Ahamed NU. Machine learning in lung sound analysis: A systematic review. *Biocybern Biomed Eng.* 2013;33(3):129-35.
5. Yahiaoui A, Er O, Yumusak N. A new method of automatic recognition for tuberculosis disease diagnosis

using support vector machines. *Biomed Res.* 2017;28(9):4208-12.

6. Papers with Code: The latest in Machine Learning, Browse State-of-the-Art Image Classification. Available from: <https://paperswithcode.com/task/image-classification>

7. Myszczyńska MA, Ojames PN, Lacoste AM, Neil D, Saffari A, Mead R, et al. Applications of machine learning to diagnosis and treatment of neurodegenerative diseases. *Nat Rev Neurol.* 2020;16(8):440-56.

8. Ibrahim AU, Ozsoz M, Serte S, Al-Turjman F, Yakoi PS. Pneumonia classification using deep learning from chest X-ray images during COVID-19. *Cogn Comput.* 2021;13:1317-28.

9. Deepan P, Sudha LR. Deep Learning and its Applications related to IoT and Computer Vision. In: *Artificial Intelligence and IoT: Smart Convergence for Eco-friendly Topography.* Singapore: Springer Nature; 2021. p. 223-44. Available from: [https://doi.org/10.1007/978-981-33-6400-4\\_11](https://doi.org/10.1007/978-981-33-6400-4_11)

10. Islam SR, Maity SP, Ray AK, Mandal M. Deep learning on compressed sensing measurements in pneumonia detection. *Int J Imaging Syst Technol.* 2022;32(1):41-54.

11. Ghantasala GP, Sudha LR, Priya TV, Deepan P, Vignesh RR. An Efficient Deep Learning Framework for Multimedia Big Data Analytics. *Multimedia Comput Syst Virtual Reality.* 2021;99:1-12.

12. Ibrahim DM, Elshennawy NM, Sarhan AM. Deep-chest: Multi-classification deep learning model for diagnosing COVID-19, pneumonia, and lung cancer chest diseases. *Comput Biol Med.* 2021;132:104348.

13. Bharati S, Podder P, Mondal MRH. Hybrid deep learning for detecting lung diseases from X-ray images. *Inform Med Unlocked.* 2020;20:100391.

14. Mahdy LN, Ezzat KA, Elmousalimi HH, Ella HA, Hassanien AE. Automatic X-ray COVID-19 lung image classification system based on multi-level thresholding and support vector machine. *medRxiv [Preprint].* 2020. Available from: <https://doi.org/10.1101/2020.03.30.20047787>

15. Mahbub MK, Biswas M, Gaur L, Alenezi F, Santosh KC. Deep features to detect pulmonary abnormalities in chest X-rays due to infectious diseases: COVID-19, pneumonia, and tuberculosis. *Inform Sci.* 2022;592:389-401.

16. Qaqos NN, Kareem OS. COVID-19 diagnosis from chest X-ray images using deep learning approach. In: *2020 International Conference on Advanced Science and Engineering (ICOASE); 2020 Dec 23-24; Duhok, Iraq.* New York: IEEE; 2020. p. 110-6.

17. Haghanifar A, Majdabadi MM, Choi Y, Deivalakshmi S, Ko S. Covid-cxnet: Detecting COVID-19 in frontal chest X-ray images using deep learning. *Multimed Tools Appl.* 2022;81:31-51.

18. Okolo GI, Katsigiannis S, Althobaiti T, Ramzan N. On the Use of Deep Learning for Imaging-Based COVID-19 Detection Using Chest X-rays. *Sensors.* 2021;21(17):5702.

19. Kaggle Datasets. COVID-19 Detection X-ray Dataset. Available from: <https://www.kaggle.com/darshan1504/covid19-detection-xray-dataset>

20. Kaggle Datasets. Lungs Dataset. Available from: <https://www.kaggle.com/muhammadrizkyperdana/lungs-dataset>

21. Kaggle Datasets. Chest X-ray Pneumonia. Available from: <https://www.kaggle.com/paultimothymooney/chest-xray-pneumonia>

22. Kaggle Datasets. Chest X-ray Pneumonia, COVID-19, Tuberculosis. Available from: <https://www.kaggle.com/jtiptj/chest-xray-pneumoniacovid19tuberculosis>

23. Kaggle Datasets. Chest X-ray 14 Lungs Cropped. Available from: <https://www.kaggle.com/iamsuyogjadhav/chest-x-ray-14-lungs-cropped>

24. Kaggle Datasets. Tuberculosis (TB) Chest X-ray Dataset. Available from: <https://www.kaggle.com/tawsifurrahman/tuberculosis-tb-chest-xray-dataset>

#### **FINANCING**

The authors did not receive financing for the development of this research.

#### **CONFLICT OF INTEREST**

The authors declare that there is no conflict of interest.

#### **AUTHORSHIP CONTRIBUTION**

*Conceptualization:* Jyothi N M, Umme Najma.

*Data curation:* Savitha S, Umme Najma, Kalai Vani Y S.

*Formal analysis:* Jyothi N M, Tirumalasetti Lakshmi Narayana, Savitha S.

*Research:* Jyothi N M, Hridaynath Pandurang Khandagale, Kalai Vani Y S.

*Methodology:* Jyothi N M, Umme Najma.

*Project management:* Jyothi N M, Hridaynath Pandurang Khandagale.

*Supervision:* Savitha S.

*Validation:* Hridaynath Pandurang Khandagale.

*Display:* Kalai Vani Y S.

*Drafting - original draft:* Umme Najma.

*Writing - proofreading and editing:* Jyothi N M.